Figure S1. Comparison of control and *Lactobacillus rhamnosus* group and results of pro-inflammatory cytokine expression analyzed by RT-qPCR in mice. (A) H&E staining for colon tissues of mice stained with H&E in control and *Lactobacillus rhamnosus* group (magnification, x200). (B) mRNA levels of pro-inflammatory genes for control and *Lactobacillus rhamnosus* group. (C) The relative gene expression of IL-1β, IL-6, TNF-α and IFN-γ was detected by RT-qPCR and the data were generated from colon tissues. Data are presented as the means ± SEM of at least 3 repeated experiments. *P≤0.05, **P≤0.01. ns, not significant; *F. nucleatum*/*F.n.*, *Fusobacterium nucleatum*; *L.r.*, *Lactobacillus rhamnosus*; DSS, dextran sulfate sodium.

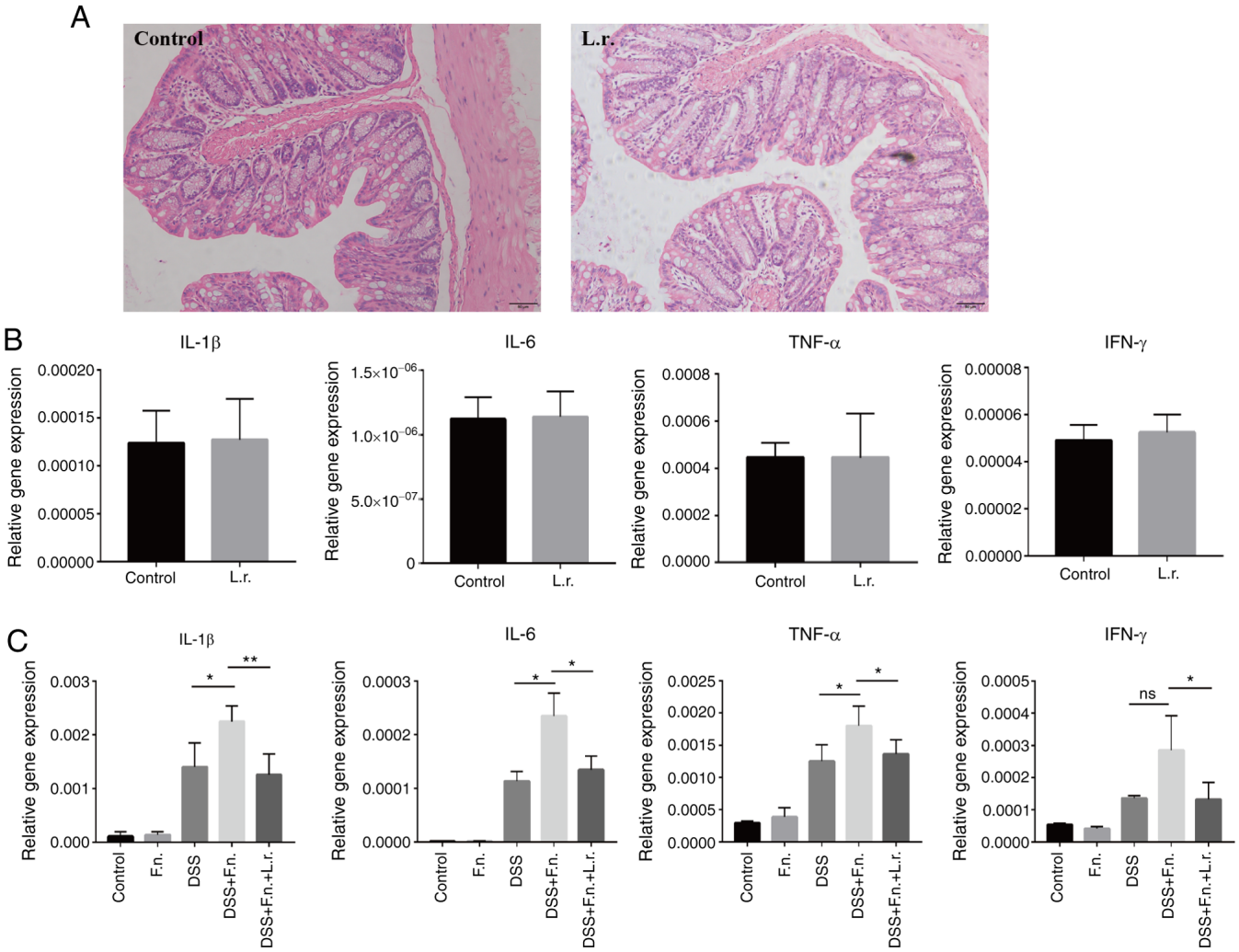

Figure S2. Results demonstrating that *Lactobacillus rhamnosus* increases autophagy inhibited by *F. nucleatum* infection *in vivo*. (A) Histogram of relative expression of LC3B and SQSTM1/p62 immunostaining. (B) The relative gene expression of Atg7, Beclin1 and Atg16L1. The data were generated from colon tissues. Data are presented as the means ± SEM of at least 3 repeated experiments. $^{*}P \leq 0.05$, $^{**}P \leq 0.01$. *F. nucleatum*/*F.n.*, *Fusobacterium nucleatum*; *L.r.*, *Lactobacillus rhamnosus*; DSS, dextran sulfate sodium.

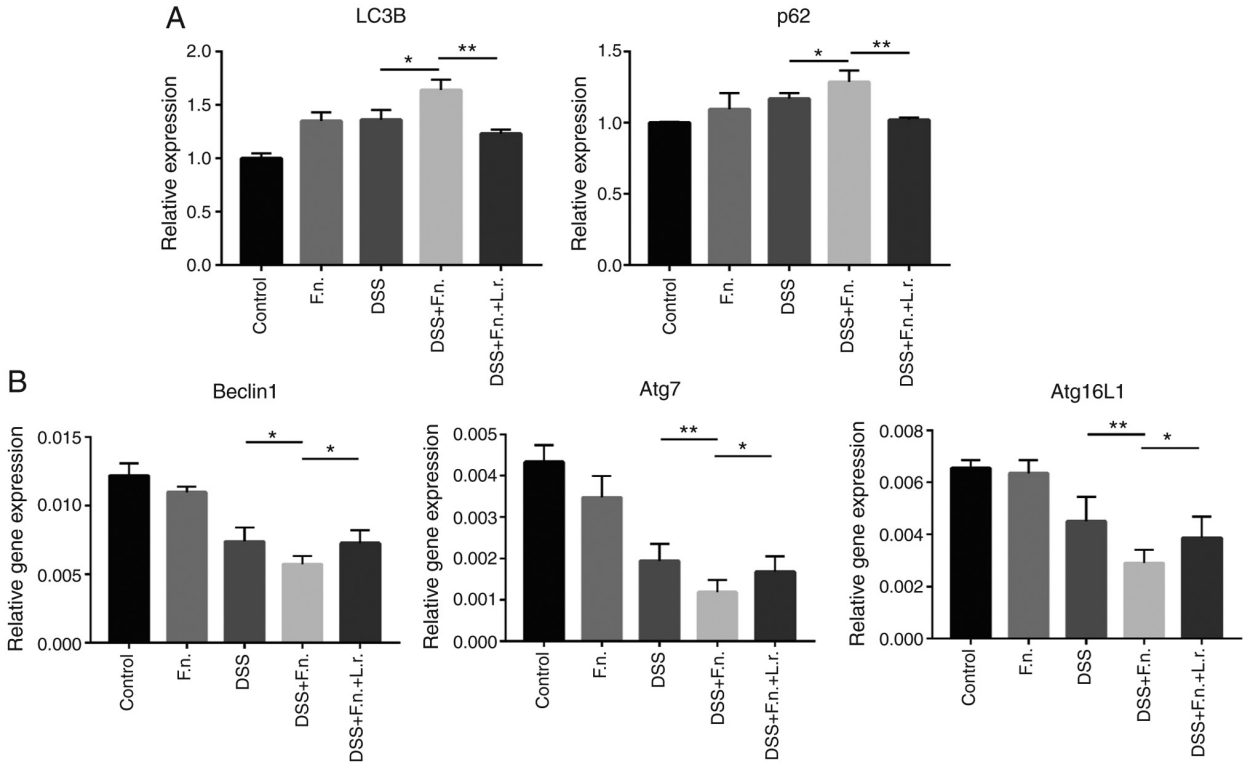

Figure S3. Statistical analysis of the western blots in Fig. 6C and D illustrating that *Lactobacillus rhamnosus* restores the impaired autophagic flux via AKT/mTOR pathway. (A and B) Histograms of relative expression of p-mTOR, p-p85 and p-AKT in Fig. 6. *P≤0.05, **P≤0.01, ****P<0.0001. ns, not significant; *F. nucleatum*/*F.n.*, *Fusobacterium nucleatum*; *L.r.*, *Lactobacillus rhamnosus*; DSS, dextran sulfate sodium.